The Optics of the Compound Eye of the Honeybee (*Apis mellifera*)

FRANCISCO G. VARELA and WAYNE WIITANEN

From the Biological Laboratories, Harvard University, Cambridge, Massachusetts 02138

ABSTRACT The optical system of the compound eye of the worker honeybee, as a representative of the closed-rhabdom type of eye, was investigated and its function analyzed. Measurements of refractive indices of the elements of the optical system were made with an interference microscope. With the use of the resulting measurements, the optical system was analyzed by means of a ray-tracing procedure implemented for the IBM 7094 digital computer, and by means of the Gaussian thick lens formulae. The more detailed results of the ray-tracing technique were used for further analyses. Direct visual confirmation of the focal point was obtained. The rhabdom and the surrounding zone of lower refractive index act together as a wave guide, as demonstrated by the presence of several wave guide modes in the rhabdom. An admittance function was defined as the percentage of the rays reaching the rhabdom with respect to those entering the ommatidium. Good agreement with experimental results was found. The characterization of the visual field of an ommatidium by means of an admittance function permits the analysis of the influence of different stimuli on the eye.

INTRODUCTION

The compound eye is made up of many small units called ommatidia, each ommatidium containing an optical system and seven or eight receptor cells (retinula cells). The visual pigments of the retinula cells are presumed to be in a membranous structure called the rhabdomere (9). In the insects, rhabdomeres from several retinula cells may fuse to form a central, closed rhabdom; but in the Diptera and certain of the Heteroptera there is no fusion, and the rhabdomeres remain isolated from one another. This spatial isolation permits each retinula cell to act as an individual receptor. Open-rhabdom eyes have been studied in detail by a number of workers (25, 4, 16, 18, 19; see reference 11 for a recent summary) who have demonstrated an elaborate optical system and a complex pattern of nervous connections (retina-lamina projections). Because of the marked anatomical differences between the two types of eye, it is not possible to make a direct comparison between them. Instead, each type of eye must be studied as a separate entity. Recently Varela and Porter[1] have

[1] Varela, F. G., and K. R. Porter. 1969. *J. Ultrastruct. Res.* **29**: 236.

investigated the fine structure of the ommatidia of the worker honeybee (*Apis mellifera*), and with the help of their data we examined the optics of the honeybee's eye as a representative of the closed-rhabdom type.

Morphology The optical apparatus of a bee's ommatidium (Fig. 1) consists of a cuticular lens, a crystalline cone, and principal pigment cells. The cuticular lens is a laminar, chitinous, transparent structure secreted by the principal pigment cells. Beneath the lens lies the crystalline cone which extends downwards for about 100μ. Its diameter decreases from about 20μ near the lens to about 4μ where it meets the rhabdom. The crystalline cone is secreted by four cells and, in the adult, four parts to the cone can be distinguished under the electron microscope. In vivo the cone is quite gelatinous and is covered by a membrane. Two principal pigment cells, forming a tight envelope around the crystalline cone, increase in cytoplasmic volume as the crystalline cone decreases in diameter so that the whole structure remains roughly cylindrical. In the lower third the cytoplasm of the principal pigment cells contains pigment granules and pigmentous substances, similar to those found in the long pigment cells, these serving to isolate the individual ommatidia throughout the retina. Unlike the eyes of some nocturnal moths, bee eyes show no pigment migration.

Each retinula cell is about 350μ long and gives rise to an axon in its distal portion which synapses with second-order neurons, forming the lamina ganglionaris of the optic lobe. Masses of microvilli arise along most of the length of the inner wall of the retinula cells to form the rhabdomeres. The eight retinula cells group themselves into pairs, and within each pair the microvilli all lie parallel to one another. Each pair of retinula cells lies in one quadrant of the almost circular rhabdom, and for this reason the microvilli of adjacent quadrants are perpendicular to one another. Near the zone where the microvilli arise the cavities of the endoplasmic reticulum are enlarged to form cisternae of various dimensions which collectively make up the inner zone.

METHODS AND MATERIALS

Determination of Refractive Indices and Structural Dimensions of Ommatidia Only worker bees from local colonies were used. The animals were decapitated, the head bisected sagittally, and the pieces frozen in a drop of water on dry ice. The specimens were cut at 10–15 μ on a microtome-cryostat (International Harris, Model CT) at about -25°C. The slices were mounted in either glycerin or insect Ringer, and quick melting was avoided. All measurements were taken immediately after mounting.

For measurements of refractive indices a Zeiss interference microscope equipped with a Sénarmont compensator was used. This instrument measures the phase-retarding properties of a structure by transferring the background darkness to the structure in question through a rotation of the analyzer. The angle of rotation is

then converted to a phase difference by means of a conversion factor. The index of refraction of the structure may then be computed from the formula

$$n_{\text{structure}} = \frac{\Delta\varphi}{d} + n_{\text{medium}}$$

where d is the thickness of the section, and $\Delta\varphi$ is the phase difference. The indices of refraction for the two mounting media used are

$$n^{546}_{\text{glycerin}} = 1.4762, \text{ and } n^{546}_{\text{water}} = 1.3347.$$

All measurements were made with 546 nm light and a minimum of 25 measurements was taken for each structural element. Glycerin was used as the mounting medium only in the measurement of the refractive index of the corneal elements.

Other preparations were made using the Smith and Farquhar tissue sectioner (Sorvall TC-2). Heads were embedded in agar at about 35°C, and 10–20 μ sections were cut after the agar had hardened. The yield was extremely low, but some measurements could be made to check for possible effects of freezing on the indices of refraction. Observations on frozen eyes were made with the electron microscope, following a technique described elsewhere.[1]

The radii of curvature of the lens surfaces were measured by using the formula

$$r = \frac{h^2 + d^2}{2h}$$

where $2d$ is the length of any chord to the arc of a great circle whose radius of curvature is r, and h is the height of the perpendicular bisector of the chord, measured between the chord and the point of contact of the bisector with the arc. The radius used was the average of all the maximum radii obtained from each ommatidium measured.

Methods for Observing Wave guide Modes and the Position of the Focal Point Slices of several eyes were made with a sharp razor blade and mounted with the corneal side facing the condenser in a moist chamber between two cover slips. The space inside the chamber was commensurate with the thickness of the slice ensuring that the ommatidia were not compressed. The preparation was observed under a microscope illuminated by a microbeam produced by placing a specially made 1 μ electron microscope aperture (C. W. French & Co., Weston, Mass.) on top of the microscope condenser, one-half mm away from the eye. The illumination used was 546 nm light. By moving the preparation it was always possible to find a position at which the orientation of the optical axes of some ommatidia coincided with the axis of the beam, fully illuminating the rhabdoms. These areas were photographed and the resulting prints inspected.

This same setup was used to locate the focal point within the optical system, as described below.

RESULTS

Determination of Optical Constants

Fig. 1 is a schematic representation of the optical system on which the various indices of refraction have been placed. Each of the elements will be discussed separately.

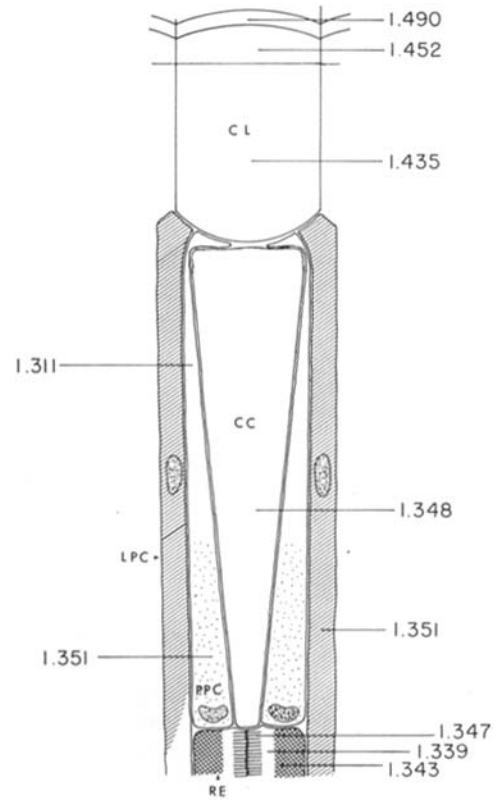

FIGURE 1. Diagrammatic representation of an ommatidium from a bee's eye showing the indices of refraction for the various structural elements. Abbreviations, *CL*, cuticular lens; *CC*, crystalline cone; *PPC*, principal pigment cells; *LPC*, long pigment cells; *RE*, retinula cells.

(a) *Cuticular lens* Axial sections of the cuticular lens reveal the presence of three layers differing in refractive index as shown in Figs. 2 and 3. The layers are coaxial and appear in longitudinal sections as three overlapping zones, each with its own curvature. The lengths and refractive indices are collected in Table I. From this description it is clear that the cuticular lens of the bee is not a "lens cylinder" as is often ascribed to compound eyes, without qualification, by some authors (Wigglesworth (26), Imms (12) for example) based on Exner's studies of *Lampyris* (7).

(b) *Crystalline cone and pigment cells* Fig. 4 shows that the crystalline cone

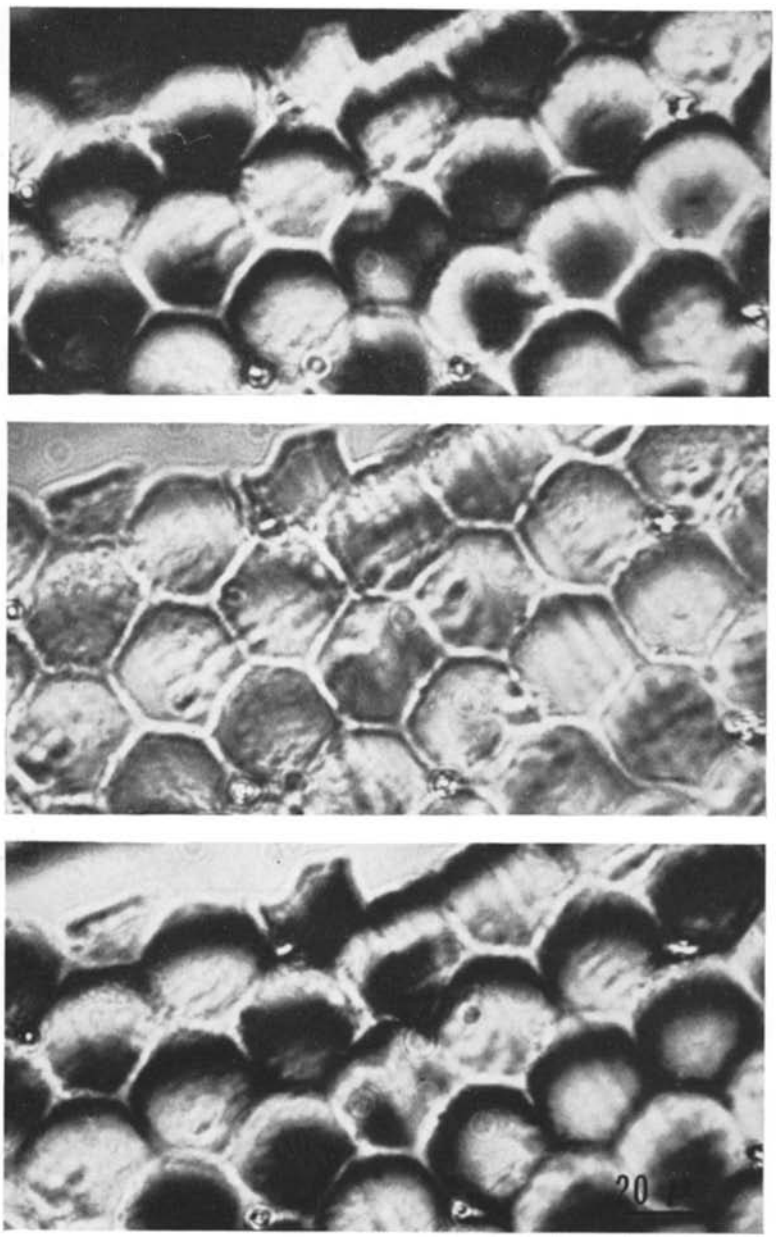

FIGURE 2. Cross-section through the cuticular lens showing the results of the index of refraction measurement technique. Upper figure, background is extinguished by the action of the compensator. Middle figure, transition phase showing a typical interference microscope image. Lower figure, background darkness has been transferred to the lenses.

is optically homogeneous in spite of being formed from four parts. The irregularities seen in the micrograph are caused by distortions, introduced during sectioning, due to the gelatinous nature of the cone. Its refractive index is 1.3477 ($\pm$0.0004 SD). The principal pigment cells have a refractive index which differs from that of the crystalline cone. There is a continuous variation in the upper part of the principal pigment cells and it is difficult to assign

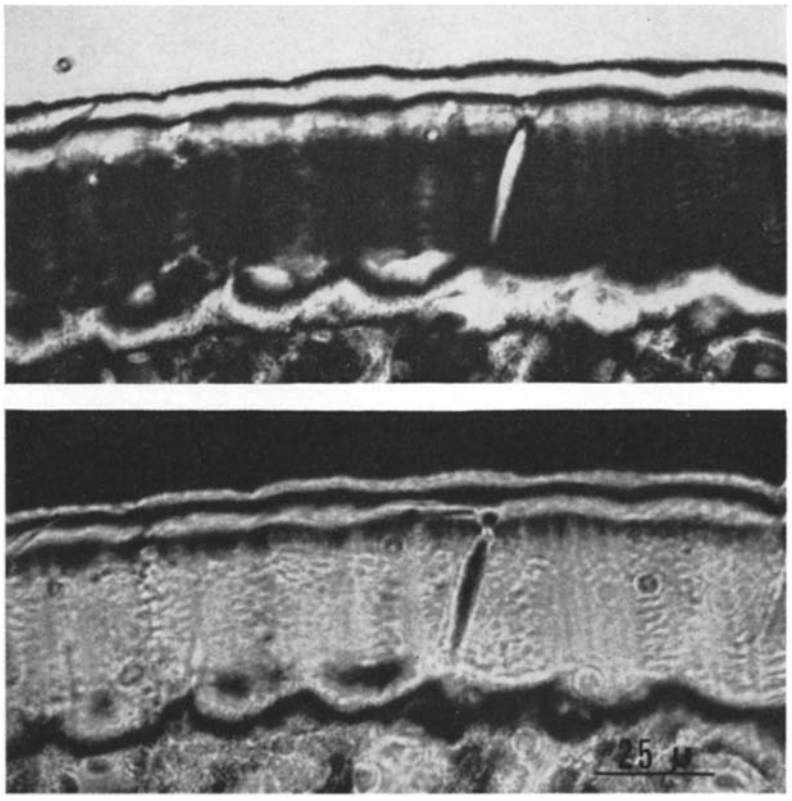

FIGURE 3. Longitudinal sections through the cuticular lens showing the transference of the background to the refracting structures. Three zones with differing refractive indices (and intermediate zones) can be distinguished.

particular values to precise levels, except at the extremes of the cells. Some indication of this gradient can be given: the refractive index in the upper middle part is 1.3114 ($\pm$0.0065)[2], and throughout the lower half of the cell it is 1.3514 ($\pm$0.0005). Thus, the lower part of the crystalline cone is surrounded by a medium having a higher refractive index than its own. The long pigment

[2] It is anomalous to find the refractive index lower than that of water (1.333). This could be explained by the fact that the tissue might have been partially frozen at the time of observation (the refractive index of ice is 1.309).

cells, surrounding the principal pigment cells, show a uniform refractive index throughout, which is indistinguishable from that of the lower part of the principal pigment cells (1.3514).

(c) *Retinula cells* The morphology of the inner zone of the receptors suggests that this part of the cytoplasm might have a lower refractive index than has the rhabdom, due to the presence of expanded cisternae of the endoplasmic reticulum.[1] An annulus, related to the inner zone, was observed around

TABLE I

DIMENSIONS AND REFRACTIVE INDICES OF THE LAYERS OF THE CUTICULAR LENS

Zone	Length	Index of refraction (±SD)
	μ	
1	8–10	1.4896 (±0.0020)
2	10–12	1.4521 (±0.0015)
3	28–30	1.4350 (±0.0006)

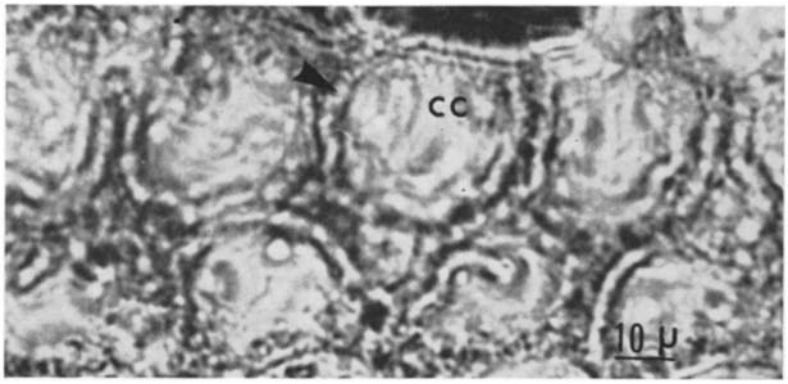

FIGURE 4. Cross-section through the crystalline cone showing an annulus (arrow) representing the principal pigment cells. *CC*, crystalline cone.

the rhabdom with interference microscopy, as shown in Fig. 5. The refractive indices of the retinula cells (Table II) indicate that the rhabdom could act as a wave guide, as was verified experimentally (see below).

Curvatures of the Cuticular Lens The radius of curvature of the first (outside) surface of the cuticular lens (surface 1 in Fig. 6 A) was found to be 43 (±3.2) μ. This value was also used for the radius of curvature of the second refracting surface in the model (surface 2 in Fig. 6 A). For the inner curved surface the radius of curvature was found to be 22 (±3.5) μ (surface 4 in Fig. 6 A).

Discussion It is interesting to note that our results are similar to those obtained by Seitz (19) in the blowfly (*Calliphora erythrocephala*) in many respects. Not only are the values for the refractive indices similar, but also some structural features of the optical system are similar; in particular: a three-layered cuticular lens, a crystalline cone surrounded by cells of higher refractive index, and a rhabdom of higher refractive index than its surroundings.

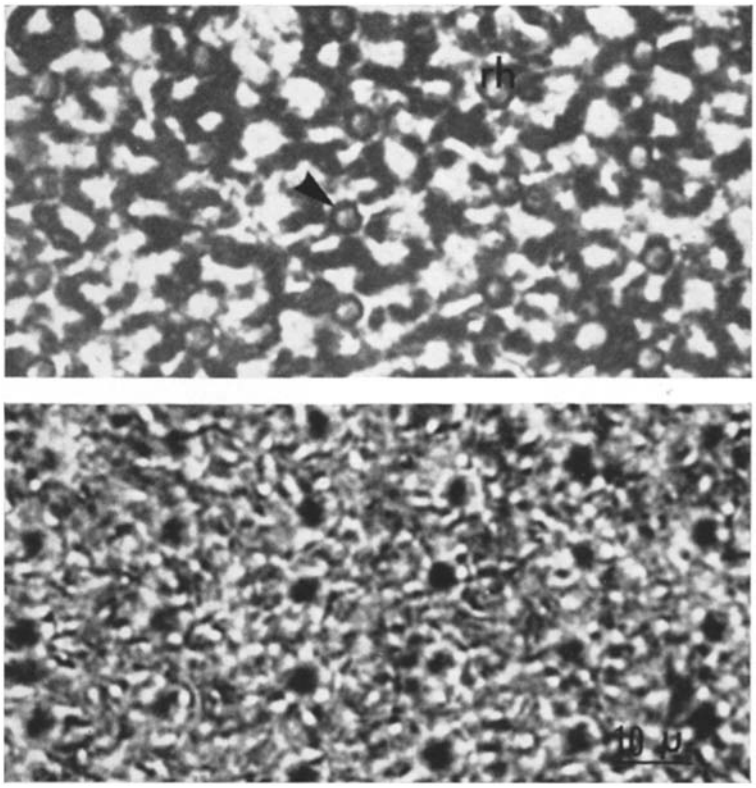

FIGURE 5. Cross-section through many ommatidia cut at the level of the rhabdom. An annulus representing an inner zone of lower refractive index than the rhabdom is shown at the arrow. The lower picture shows transference of darkness from the background to the rhabdom. *rh*, rhabdom.

It has been suggested that the process of freezing would introduce some distortion into the refractive index measurements. This was not observed to be true here, because comparison between frozen and fresh tissue showed that the differences in refractive indices measured with the two methods could not be distinguished from measurement error (third and fourth decimal places). Furthermore, the morphology of frozen tissue could be distinguished from that of normal tissue only by minor distortions (some asymmetry of the rhabdom, and absence of microtubules).

Analysis of the Optical System by Ray-Tracing Techniques

A ray-tracing program for the IBM 7094 digital computer was used to obtain exact data about the disposition of rays within the optical system. The method used relies on an algebraic description of the shape of the refracting surfaces, a knowledge of the indices of refraction for the various volumes of material bounded by the refracting surfaces, and a specification of the rays to be traced. The refracting surfaces are described in a general algebraic format by providing the ray-tracing procedure with the coefficients (A, B, C, D, E, F, G) of the equation

$$Ax^2 + By^2 + Cz^2 + Dx + Ey + Fz = G$$

which is suitable for describing any second-degree surface. Indices of refraction must be provided for the media which follow each of the surfaces. The results obtained for each ray are: its point of intersection with each refracting

TABLE II
REFRACTIVE INDICES OF THE ZONES OF A RETINULA CELL

Structure	Index of refraction (±SD)
Rhabdom	1.3468 (±0.0011)
Inner zone	1.3388 (±0.0009)
Outer zone	1.3432 (±0.0019)

surface, the transmittance, reflectance, energy densities of transmitted and reflected waves, the intensities of the transmitted and reflected waves, and the directional cosines of the refracted ray as it leaves the surface. If a ray strikes an aperture, is not refracted, or else takes a virtual path, the abnormality is noted and the next ray is selected for processing. When there is an intersection of a ray with the optical axis, the point of intersection is reported, which facilitates locating the focal point.

Fig. 6 A shows the model which was used for the ray-tracing studies, and Fig. 6 B shows the paths taken by certain rays within the optical system. The ray numbered 1 is 8μ above and parallel to the optical axis. It crosses the axis within the crystalline cone at the point labeled 1. The ray numbered 2 is nearer the optical axis and it crosses the axis inside the cone at point 2. From these ray paths it appears that as the rays come closer and closer to the optical axis their points of intersection with it will approach the point labeled 3, the focal point of the system.

The computer program was originally written by William Webb of the Goodyear Aerospace Corporation based on a method devised by G. H. Spencer in an IBM

Research Note (24), converted to the Fortran IV programming language, and further expanded for our requirements.[3] In order to verify that the program was functioning correctly, two test cases were run using data from Jenkins and White (14). We found that the results of the program agreed with their solutions with at least as much accuracy as the published calculations showed.

Analysis by the Gaussian Thick Lens Formula It is important to compare the results of the ray-tracing studies with those obtained by use of the Gaussian

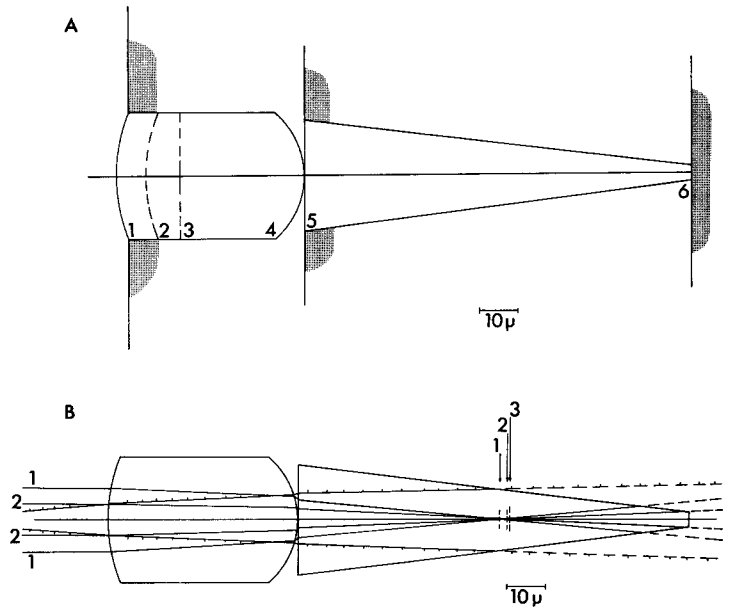

FIGURE 6. A, diagram of the optical system used by the ray-tracing technique. Numbers indicate refracting surfaces and cross-hatching shows the position of the apertures. B, results of the ray-tracing technique using the model from A. The ray numbered 1 is 8 μ above the optical axis and parallel to it. This ray crosses the optical axis within the crystalline cone at the point marked 1. Ray 2 is parallel to the optical axis at a distance of 4 μ from it, and crosses it within the crystalline cone at the point marked 2. The focal point of the system is at the point marked 3, about 34 μ above the rhabdom. The divergent ray, indicated by the lines with dots on them, is refracted into the principal pigment cell (the actual refraction is not shown).

thick lens formulae because of the latter's widespread use in the analysis of biological optical systems.

In order to apply the thick lens formulae we computed an average index of refraction for the cuticular lens by means of a weighted average formula:

$$d = \sum_i d_i \quad \text{and} \quad \bar{n} = \frac{1}{d} \sum_i n_i \, d_i$$

[3] Wiitanen, W. In preparation.

where d_i is the approximate thickness of zone i, and n_i is the refractive index of that zone. For the bee we found that $\bar{n} = 1.4530$. The Gaussian thick lens formulae, taken from Born and Wolf (3), were programmed in Fortran IV for the IBM 7094 and the program was verified against the same test cases used for the ray-tracing program.

The results of applying the thick lens formulae are illustrated in Fig. 7. The principal planes are labeled H and H', and the (secondary) focal point is so labeled. There is a slight difference between the results obtained with the two methods. Ray tracing placed the focal point (for paraxial rays and using the trilaminar lens) 60μ below the lower surface of the cuticular lens. On the other hand the thick lens formulae put the focal point 63.7 μ below the lower surface of the lens.

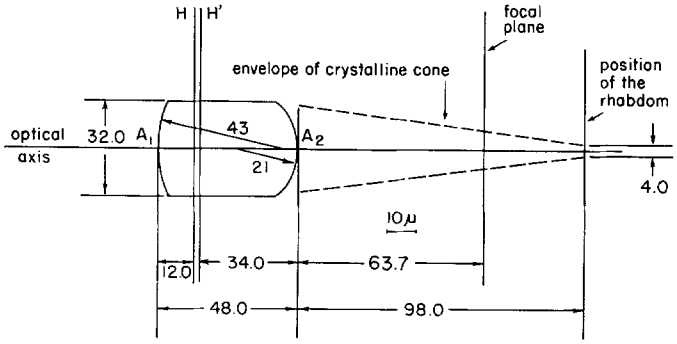

FIGURE 7. Diagram showing the results obtained from the thick lens formula. H and H' are the principal planes. All measurements are in microns. Compare with Fig. 6.

Discussion One possible source of error in the location of the focal point lies in the values of the refractive indices of the various parts of the optical system. Therefore, a series of ray-tracing studies was made in which the indices of refraction of the lens, the cell material between the lens and the face of the crystalline cone, and the crystalline cone itself were varied, for a total of 64 different combinations. The index of refraction for each of the elements was varied by steps of 0.1 (equivalent to about 100–500% observational error) above and below our measured values. The results were difficult to interpret but we ascertained that the percentage of error introduced into the location of the focal point, with respect to that of the model, was less than the largest per cent observational error in any of the three elements named. On the basis of the small standard deviations indicated in our refractive index data we believe that an observational error of less than 1% is reasonable, and that the effect of such an error on the position of the focal point is negligible.

A second important source of error lies in variations introduced into refractive index measurements by inaccurate determination of section thickness.

To evaluate this source of error, sections from a plastic block of known refractive index were cut in the same microtome so that any variation in the refractive index of the section was attributable only to variations in section thickness. In this way we ascertained that the variations in thickness lay (on the average) in the range 5–8%. Variations in this range introduce an error in refractive index of a fraction of a per cent. Consequently, variations in section thickness had a negligible influence on the position of the focal point.

Finally, variations in the radii of curvature for the refracting surfaces of the corneal lens were considered as potential sources of error in focal point position. A series of ray-tracing studies was done in which the values of the radii of curvature were changed from the mean values by $\pm 10\%$. A 10% variation in the radius of curvature of the rear surface (surface 4 of Fig. 6 A) introduced an error of about $1\frac{1}{2}\%$ in the position of the (mean) focal point. The front surface was found to be more sensitive: a 10% variation in the radius of curvature (surfaces 1 and 2 in Fig. 6 A) introduced a $6\frac{1}{2}\%$ error into the position of the focal point.

In view of these points we conclude that errors in refractive indices and radii of curvature in our measurements are not likely to be important sources of error in the determination of the focal point.

The main difference between the thick lens formulae and the ray-tracing method is that the thick lens formulae do not account for the crystalline cone as an optical element, but merely use the refractive index of the cone as the refractive index of the medium which follows the second surface of the lens. In addition, the trilaminar structure of the cuticular lens cannot be taken into account, and an averaged representation must be used. Another difference is that the thick lens formulae are unable to provide information about the precise trajectories of the rays as they pass through the system, nor are they able to provide information about the intensities of the rays as they pass through each refracting element in the system. A final difference, of lesser importance, is that the thick lens formulae use an approximation to the sines of the angles of incidence and refraction (Snell's law). The fact that the focal point determined by ray tracing and by the thick lens formulae, applied to two rather different optical systems, yields nearly identical results is an amusing coincidence.

We want to emphasize that the ray-tracing method is not only more accurate than the thick lens formulae but also has the added advantage of providing us with the path which each ray takes through the optical system, and the intensity of each ray within the system. From the paths we are able to determine the distribution of rays that enter the rhabdom and in this way we can analyze how the incoming energy is transmitted through the optical system (see below).

The fact that the focal point is above the level of the rhabdom has an im-

portant implication in that it narrows the field of view of an ommatidium. In fact, the light that has been concentrated at the focal point will diverge progressively as it gets closer to the rhabdom, and eventually most of these diverging rays will hit the sides of the crystalline cone and be refracted into the principal pigment cells for subsequent extinction. This happens because the refractive index of the principal pigment cells, in their lower parts, is higher than the refractive index of the crystalline cone, meaning that if a ray is to have any effect on the rhabdom it must traverse the optical system without hitting the lateral boundaries of the crystalline cone or any other element of the optical system.

Verification of the Location of the Focal Point The position of the focal point above the rhabdom was verified experimentally. Fresh slices of eyes were cut perpendicular to the axis of some central ommatidium with a razor blade, and were mounted as described in the Methods section. By taking a section near the surface of the eye, all elements of the optical system were present in the slice (each of the elements was cut at several different levels due to the curvature of the eye). By moving the preparation on a microscope stage, it was observed that when a light beam collimated to a 1 μ diameter fell on the zone of the section containing just the lens, it appeared to be filled uniformly with light. As various levels of the crystalline cone were moved under the microscope objective, the diameter of the beam was seen to decrease to a minimum and then to increase again, indicating that the focal point was within the crystalline cone. Technical difficulties precluded more accurate measurements, but there could be no doubt that the focal point was above the rhabdom and was probably near the middle of the crystalline cone.

Optimum Size for an Ommatidium If it is advantageous to narrow the field of view to improve resolution, why not achieve the same effect by reducing the size of each ommatidium? The limitation of such an approach is that reduction in size introduces losses due to diffraction. This fact makes it pertinent to ask how one can get an estimate of the optimum size of an ommatidium (10, 2). Following the approach of Feynman et al. (8) we see that the greater the number of facets distributed over the surface of the eye the better the resolution should be. This packing defines a number, θ_p, the angular size of a facet, by the formula

$$\theta_p = d/r$$

where θ_p is in radians, d is the facet diameter, and r is the radius of the eye. As the facet size decreases, the effects of diffraction increase and mask the acuity gained by reducing the size of the facets. Diffraction effects define an angle, θ_d, below which the resolution losses due to diffraction become significant, by

the well-known formula

$$\theta_d = 1.2\lambda/d$$

where θ_d is in radians, and λ is the wavelength of light. From measurements on the whole eye of the honeybee we found $r = 1.22$ mm. In order to find the optimum d we have

$$\frac{\partial}{\partial d}(\theta_d + \theta_p) = 1/r - 1.2\lambda/d^2 = 0$$

which has the solution

$$d = (1.2r\lambda)^{1/2}$$

By inserting the values for λ and r ($\lambda = 0.546\ \mu$), we find that $d = 29\mu$ which agrees well with the observed value of 32 μ. Thus, it appears that the eye strikes a balance between acuity and diffraction losses.

Because the crystalline cone becomes narrow as it nears the rhabdom it is possible that Fraunhofer diffraction losses, due to the presence of the small aperture made by the pigment cells surrounding the crystalline cone, may be significant. Determination of the intensity pattern at the focal point was simplified by the elegant development found in Born and Wolf (3). By evaluating their formulae for u and v we found that $u = 0.0$ and $v = 0.98$. By locating these points on their graph we found that the principal maximum as well as half of the second maximum of intensity was included within the crystalline cone at the focal point. This assures us that the crystalline cone is not significantly reducing the amount of light reaching the focal point due to the slope of its sides. We were unable to do an analysis of losses due to diffraction at the crystalline cone-rhabdom junction.

The ray-tracing procedure also gives the intensities of the transmitted rays as they leave each refracting surface. The calculation is performed using the formulae of Born and Wolf (3) found on pages 36–45. Results of analyses using these formulae show that the intensity of the rays transmitted to the rhabdom is all at 95% of the intensity of the incident rays.

The Rhabdom As a Wave Guide

The fact that the rhabdom acts as a wave guide effectively obviates the problem of imaging, in the conventional sense. This section will deal with evidence that we think supports this view.

A necessary condition for a structure to be a wave guide is that the dielectric constant (the square of the real part of the complex refractive index, assuming that the relative magnetic permeability of the medium is 1) of the surrounding

medium be lower than that of the wave guide itself. This is the case in the bee's ommatidium where, as described before, the inner zone of the retinula cells provides such a surrounding area (in fiber optics terminology, the cladding) of lower refractive index for the rhabdom. It is easy to calculate the critical angle, θ_c, for this arrangement by means of the formula

$$\theta_c = \pi/2 - \arcsin(n_{\text{inner zone}}/n_{\text{rhabdom}}) = 0.109 \text{ radian } (6°15 \text{ min})$$

The value of this angle assures us that the rhabdom may act as a wave guide because the angle that the wall of the crystalline cone makes with the optical axis is similar (7°).

Basic Properties of a Wave guide Any device that constrains, or guides, the direction of propagation of incident electromagnetic radiation along a path defined by the geometry of the device is known as a wave guide. The importance of such devices in microwave engineering is well-known and their mathematical characterization has been worked out in detail (see (5) for a comprehensive treatment). We have observed the wave guide modes predicted by theory in the retinula cell-rhabdom complex of the bee's eye, as has Enoch (6) in vertebrate rods and cones.

For glass fibers it has been shown (22, 15) that the incident light waves are transmitted in distinct patterns or modes, which can be observed at the tip of the glass fiber. Their number varies according to the diameter of the fiber. From the mathematical description of the behavior of light waves in a wave guide several questions may be asked concerning: (*a*) whether or not certain wavelengths of light will be propagated down the wave guide, (*b*) what modes are present in the wave guide, (*c*) the distribution of energy in the wave guide, and (*d*) the influence of the angle of incidence of light on the wave guide modes.

Wave Guide Modes Under conditions of optimum illumination and orientation the six or seven ommatidia illuminated showed modal patterns (direct images). The types most frequently seen are shown in Fig. 8. Other modes were also seen but their classification is obscure. The presence and classification of each mode follow from a characterization of the mode, called the "cutoff parameter." This parameter (u_{nm}) is derived from studies on fiber optics (22) and must satisfy the inequality

$$u_{nm} \leq 2\pi(r/\lambda)(n_1^2 - n_2^2)^{1/2}$$

where λ is the free space wavelength of the light employed, r is the radius of the rhabdom, n_1 is the refractive index of the rhabdom, and n_2 is the refractive index of the surrounding medium (retinula cell inner zone). This cutoff parameter indicates that only certain modal patterns will be present in a

particular wave guide. By inserting the values which we have for λ, r, n_1, and n_2 for the bee's eye, we find that $u_{nm} \leq 3.4$. Accordingly the modes most commonly found will be those with a low cutoff (0.0–3.4).

Because bees have the ability to perceive the polarization of light, we examined the effect of polarized light on the wave guide modes of the rhabdom, and observed no differences between the modes obtained with polarized light and those obtained with unpolarized light, for any angle of polarization.

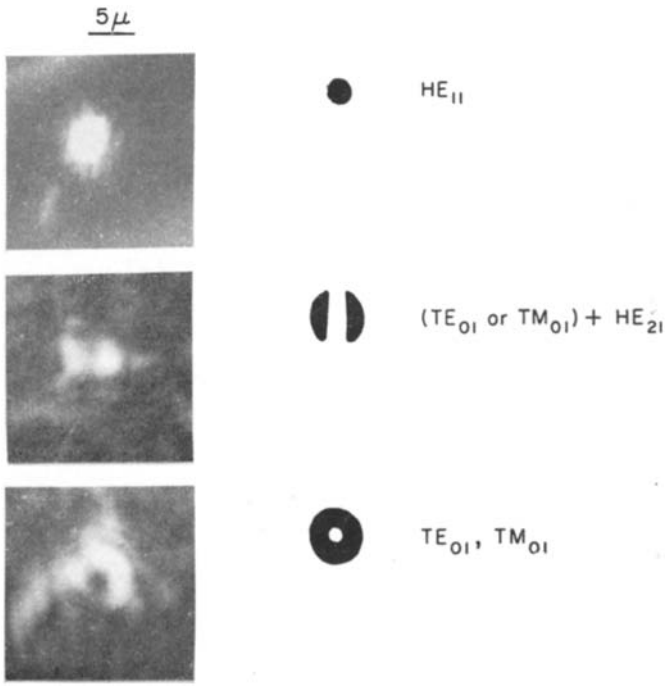

FIGURE 8. Photographs of wave guide modes observed in different sections through the rhabdoms of some ommatidia. These modes represent those most commonly found. To the right is an idealized representation of the modes with their designation according to Enoch (6).

The fact that the rhabdom acts as a wave guide has important implications for our understanding of how the receptors of an ommatidium receive incoming light. It is true that an asymmetrical light distribution can, and probably does, produce modes with asymmetrical energy distributions within a wave guide. In the case of the rhabdom such a distribution might lead to asymmetrical stimulation of the receptor cells. Nevertheless, investigations by Snitzer and Osterberg (23) on fiber optics call to our attention the fact that fibers which are large enough to support several modes will support two or more modes excited simultaneously. This implies that no single modal pattern

will be maintained by the fiber but a superposition of patterns will be, making it unlikely that any single asymmetrical mode will be dominant; and that any such possibly dominant mode would be masked by others that would not have the same energy distribution.

The same authors also point out that as a wave guide deviates from circular symmetry new modes are obtained that are linear combinations of those found in the perfectly circular wave guide. The tendency for asymmetrical modes to appear when the geometry of the wave guide is distorted is proportional to the difference in refractive indices of the core and cladding, that is, if the difference is small the tendency to shift modes is large. Our measurements show that this difference is very small for the rhabdom (0.008), indicating that the normal variations in the circularity of the rhabdom would introduce a variety of asymmetrical modes, their field patterns varying with the distortions found throughout the length of the rhabdom.

Whenever lobed patterns appeared, Snitzer and Osterberg (23) observed that the patterns would change their orientation abruptly as the wave propagated down the wave guide. This would indicate that it is unlikely for stable lobed patterns to persist throughout the length of the rhabdom even if the light distribution at the top of the rhabdom were asymmetrical. As the wavelength of the stimulating light was varied, the lobed patterns again changed their azimuthal orientation (rotation of the null line) along the axis of the wave guide. Under physiological conditions, the light being used by the bee is predominantly white and this would argue that no single wave guide mode would predominate. Lobed patterns were observed experimentally only with monochromatic light, and, for our observations of the bee's eye, the lobed patterns were not the most commonly seen ones.

Although the above reasons are not conclusive, they provide strongly suggestive evidence in support of the assumption that each ommatidium acts as a unit in light reception; that is, all the cells from one ommatidium will be excited to comparable levels regardless of any asymmetry in the distribution of the incoming light. For these reasons we will assume that the visual field of any ommatidium is circularly symmetric, and has an intrinsic ambiguity which increases with the distance of an object from the surface of the eye.

Extinction of Stray Light by Pigment Cells

Because a large percentage of the rays passing through the optical apparatus are refracted into the pigment cells it is appropriate to investigate their fates among the pigment granules. An analytical approach by means of scattering principles (12) is not possible at this time because the nature and physical parameters of the pigment granules are not known; but we can suggest how the extinction of rays refracted into pigment-containing cells might take place. Light leaving the crystalline cone must travel through three pigmented cells before it could get into the rhabdom of a neigh-

boring ommatidium. From electron micrographs of these cells we find a high pigment granule density: long pigment cells have particles whose diameters average 0.42 ($\pm$0.140) μ with a density of 2.2 particles per cubic micron; principal pigment cells have particles whose diameters average 2.33 ($\pm$1.109) μ with a density varying from 1 granule per cubic micron in the upper part of the cell to 2.2 granules per cubic micron in the lower part; and retinula cells having particles whose diameters average 0.474 ($\pm$0.123) μ with a density of 9.6 granules per cubic micron. These data indicate that there is little opportunity for a refracted light ray to enter a foreign rhabdom. We may be confident, then, that there is no significant "cross-talk" between ommatidia in the bee's eye. (Computer analyses of light extinction and light intensity distributions within the optical system are currently under study.)

Admittance Function

In order to formulate precise descriptions concerning the amount of light admitted by the lens to the rhabdom we use the concept of a lens admittance function, which is defined as the percentage of parallel rays incident on the lens that are transmitted directly to the rhabdom, with respect to the angle which the rays make with the optical axis of the lens. We determined the admittance function for the bee's eye by generating fans of rays, by means of the ray-tracing technique, that made systematically varying angles with the optical axis of the model. By finding the extremes of the parallel rays that were admitted by the lens and that reached the rhabdom for each angle of incidence, we were able to compute the percentage of the total lens surface that was active in admitting incident rays to the rhabdom. The results are plotted in Fig. 9 (see the Appendix for a precise description of the mathematics involved).

By elementary curve-fitting methods the admittance function may be approximated by the function

$$f(\theta) = 6.1\exp(-0.09\theta^2)\ \theta \text{ in degrees}$$

where θ is the angle that the rays make with the optical axis. Two observations are pertinent: (*a*) the formula shows that the maximum amount of surface admitting rays is 6.1% of the total surface (this amount decays exponentially with the square of the angle of incidence, forming a bell-shaped curve), and (*b*) the graph shows a spread of points, caused by the finite step size between successive rays (required by the computer implementation of the ray-tracing technique). The jitter could be reduced at the expense of undue amounts of printed computer output.

The triangles plotted in Fig. 9 represent data taken from the experiments of Kuiper (17) and scaled to fit our graph. They represent a measurement of the intensity of light transmitted through the rhabdom as a distant point source is swung in a circular arc away from the optical axis of an ommatidium.

The scaling and alignment of peaks are justified in view of our preceding discussion on intensity losses. The agreement of the two curves is remarkable, and implies that the per cent of lens surface is, in this case, equivalent to transmitted light intensity.

In order to study in detail the effect of the position of the focal point on the admittance function, a series of ray-tracing studies was done in which the focal point was moved upwards and downwards. Analysis of these studies showed that an upwards displacement of the focal point caused the admittance function to become "sharp" but the light-gathering efficiency was low. When

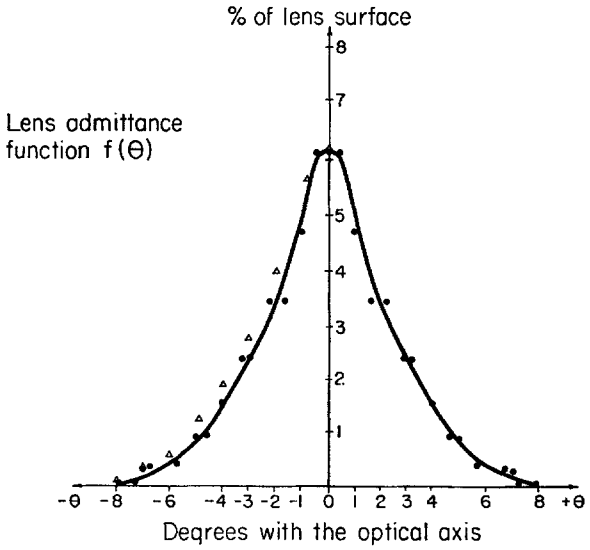

FIGURE 9. A graph of the admittance function illustrating the percentage of the total lens surface which admits rays to the rhabdom. Abscissa, angle of incidence of rays with respect to the optical axis. Ordinate, percentage of the total lens surface admitting rays. The triangles are experimental data taken from Kuiper (17) and scaled to fit our graph.

the focal point was shifted downwards, the admittance function flattened out and the light-gathering ability was increased.[4] The actual focal point position represents a compromise between a narrow angle of acceptance, with its high resolution, and a high light-gathering efficiency, with poor resolution.

[4] The following formulae characterize the shape of the three curves obtained from the analyses relating to the movement of the focal points:

$$\text{Focal point moved upwards: } f(\theta) = 4.6 \exp(-0.16\ \theta^2)$$
$$\text{Focal point in normal position: } f(\theta) = 6.1 \exp(-0.09\ \theta^2)$$
$$\text{Focal point depressed: } f(\theta) = 9.4 \exp(-0.04\ \theta^2)$$

The focal points were located at 59.0, 63.7, and 68.5 μ below the lower surface of the cuticular lens, respectively.

CONCLUSIONS

Since the work of Exner (7) it has been assumed that the optical apparatus of any compound eye could be treated adequately by the Gaussian thick lens formulae. Such an assumption fails to take into account important approximations and restrictions implicit in these formulae, and does not incorporate the particular geometry of an actual biological optical system. Other limitations of the thick lens approach are that the fate of individual rays remains unknown, and that no information concerning transmitted intensities at each refracting surface can be obtained. In order to understand the function of the different structures in the optical system it is necessary to examine the ray paths within each element. The pitfalls of the thick lens formula approach can be avoided by using the ray-tracing technique, made practical by the availability of high-speed digital computers.

We believe that the wave guide nature of the rhabdom has many important consequences. First, it indicates the way in which incoming energy is transmitted. Second, it points out that the ommatidium acts as a single unit in the reception of light intensity within its visual field. Third, it shows that the visual field of an ommatidium (as defined by the admittance function) is circularly symmetrical, and has a built-in ambiguity. Finally, the wave guide nature of the rhabdom makes considerations of imaging, in the conventional sense, unnecessary.

There are several factors that favor the grouping of compound eyes into the two classes: open and closed rhabdom types. On anatomical grounds it is apparent that the two types are different, and we have shown that there is also a functional difference. Because the rhabdomeres have fused into a single unit, the rhabdom, with a surrounding zone of lower refractive index, we have been able to demonstrate the wave guide nature of the whole complex. In the open rhabdom eye each retinula cell must be considered as a unit (4, 16). This, in turn, means that the admittance function for the open rhabdom type will differ from that for the closed rhabdom eye; the latter having a single maximum, and the former having seven maxima—one for each retinula cell (19). These facts imply that the retina-lamina projections in the two types of eyes should be different. The results of our optical analysis support the conclusion that the open and closed rhabdom eyes represent two different classes of eyes.

A quantitative analysis can begin only with the knowledge of the behavior of rays within the optical system and the role of the different structures involved. The concept of an admittance function, as a measure of the amount of light actually reaching the rhabdom compared with the amount that enters the ommatidium, is useful because it permits the analysis of the properties of

visual fields of individual ommatidia and the interactions between neighboring ommatidia. This analysis can be extended to describe the performance of the eye when confronted with complex figures.

The main object of this study has been to provide a description of the optical system of the honeybee as a representative of the closed rhabdom type of eye, and to serve as a basis for studying visual processing by means of electrical recordings from retinula cells and neurons of higher stages. It would appear that each of the eight cells of an ommatidium carry the same information about light intensity, as well as different information about polarization (20) and chromaticity (1). (This might not be the case in the drone in which electrical coupling between retinula cells has been shown [21].) How this information is disentangled by the connections of second- and higher-order neurons remains to be discovered.

APPENDIX

The percentage of the lens surface which admits rays to the rhabdom is calculated by using the fact that the ray-tracing technique provides us with two points along each ray before it reaches the first refracting surface. This allows us to derive the equation of the line representing the ray before it is refracted. Since we are dealing with a rotationally symmetric spherical lens it is easy to calculate the points of intersection of selected rays with the circle representing the lens surface. When we refer to Fig. 10 we find that the equations for the unrefracted rays are

$$\begin{bmatrix} x_{11} \\ x_{12} \end{bmatrix} = \begin{bmatrix} a_1 & 0 \\ 0 & a_2 \end{bmatrix} \cdot \begin{bmatrix} z_1 \\ z_2 \end{bmatrix} + \begin{bmatrix} x_{01} \\ x_{02} \end{bmatrix}$$

where

$$a_i = \frac{x_{1i} - x_{0i}}{z}$$

and the equation for the circle representing the lens surface is

$$(z - b)^2 + x^2 = r^2$$

where z is the distance from the origin of the optical system (100 units to the left of the first lens surface in our studies) to the center of the circle (at b), and r is the radius of the circle. By solving the equations above simultaneously for z we get the intersection of the two lines with the circle. The distance between the two intersection points is

$$d^2 = (x_2 - x_1)^2 + (z_2 - z_1)^2$$

By using the simple geometric relationship, shown to the right in the circle in

Fig. 10,

$$h = r - \left(r^2 - \left(\frac{d}{2}\right)^2\right)^{\frac{1}{2}},$$

we obtain the distance h from the chord to the arc along the perpendicular bisector of the chord. Finally we insert h into the formula which represents the surface, $A_c(r, h, d)$, of a spherical cap of diameter d and height h:

$$\theta_c = \arctan(d/2(h - r))$$

$$A_c(r, h, d) = 2\pi r^2(1 - \cos\theta_c)$$

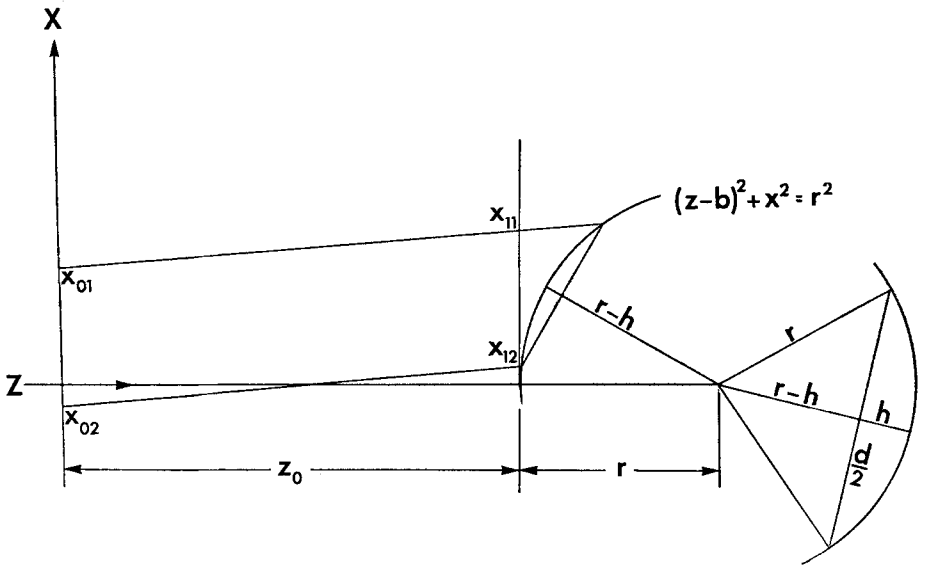

FIGURE 10. Geometrical construction for Appendix showing the lines representing rays and the circle representing the lens surface.

where r is the radius of the first lens surface. The percentage is easily obtained when the area of the facet is known ($d = 32\ \mu$, $h = 3.78\ \mu$).

We wish to thank Dr. R. A. Cone and especially Dr. T. N. Wiesel for their careful and constructive criticisms of the manuscript.

Received for publication 1 May 1969.

BIBLIOGRAPHY

1. AUTRUM, H., and V. VON ZWEHL. 1962. Die Sehzellen der Insekten als Analysoteren für Polarisertes Licht. *Z. vergl. Physiol.* **46**:1.
2. BARLOW, H. B. 1952. The size of ommatidia in apposition eyes. *J. Exp. Biol.* **29**:667.
3. BORN, M., and E. WOLF. 1965. Principles of Optics. Pergamon Press, New York. 161, 435.

4. BRAITENBERG, V. 1967. Patterns of projection in the visual system of the fly. I. Retina-lamina projections. *Exp. Brain Res.* **3**:271.
5. COLLIN, R. E. 1960. Field Theory of Guided Waves. McGraw-Hill Book Co., New York.
6. ENOCH, J. M. 1963. Optical properties of retinal photoreceptors. *J. Opt. Soc. Amer.* **53**:71.
7. EXNER, A. 1891. Die Physiologie der facettiren Augen von Kresben und Insekten. Franz Deuticke.
8. FEYNMAN, R. P., R. B. LEIGHTON, and M. SANDS. 1963. The Feynman Lectures on Physics. Addison-Wesley Publishing Co., Inc., Reading, Mass. Chapter 36.
9. GOLDSMITH, T. H. 1958. The visual system of the honeybee. *Proc. Nat. Acad. Sci. U.S.A.* **44**:123.
10. HECHT, S., and E. WOLF. 1929. The visual acuity of the honeybee. *J. Gen. Physiol.* **12**:727.
11. HORRIDGE, G. A. 1968. Interneurons. W. H. Freeman & Co., San Francisco.
12. VAN DER HULST, H. C. 1957. Light Scattering by Small Particles. John Wiley & Sons, Inc., New York.
13. IMMS, A. D. 1964. A General Textbook of Entomology. Methuen & Co., Ltd., London.
14. JENKINS, F. A., and H. E. WHITE. 1957. Fundamentals of Optics. McGraw-Hill Book Co., New York. 69, 125.
15. KAPANY, N. A., and J. J. BURKE. 1961. Fiber optics. IX. Waveguide effects. *J. Opt. Soc. Amer.* **51**:1067.
16. KIRSCHFELD, K. 1967. Die Projektion der optischen Umwelt auf das Raster der Rhabdomere im Komplexauge von Musca. *Exp. Brain Res.* **3**:248.
17. KUIPER, J. W. 1962. The optics of the compound eye. In Biological Receptor Mechanisms. J. W. L. Beament, editor. Academic Press, Inc., New York. 58.
18. MELAMED, J., and O. TRUJILLO-CENÓZ. 1968. The fine structure of the central cells in the ommatidia of dipterans. *J. Ultrastruct. Res.* **21**:313.
19. SEITZ, G. 1968. Die Strahlengang im Appositionsauge von *C. erythrocephala* (Meig.). *Z. vergl. Physiol.* **59**:205.
20. SHAW, S. R. 1967. Simultaneous recordings from two cells in the locust retina. *Z. vergl. Physiol.* **55**:183.
21. SHAW, S. R. 1967. Electrical coupling between receptors in the eye of the drone honeybee. *J. Gen. Physiol.* **50**:2480.
22. SNITZER, E. 1961. Cylindrical dielectric waveguide modes. *J. Opt. Soc. Amer.* **51**:491.
23. SNITZER, E., and H. OSTERBERG. 1961. Observed dielectric waveguide modes in the visible spectrum. *J. Opt. Soc. Amer.* **51**:499.
24. SPENCER, G. H. 1961. A general ray tracing procedure. IBM Corporation Research Paper RC-549.
25. TRUJILLO-CENÓZ, O. 1965. Some aspects of the structural organization of the intermediate retina of dipterans. *J. Ultrastruct. Res.* **13**:1.
26. WIGGLESWORTH, V. B. 1965. The Principles of Insect Physiology. Methuen & Co., Ltd., London. 188.